A STUDY ON DAMAGE PROCESSES OF A RUBBLE MOUND BREAKWATER BASED ON ADVECTION DIFFUSION EQUATION

Daiki Sakai[1] and Gozo Tsujimoto[2]

At construction sites of rubble mounds, concern often arises regarding the vulnerability of these structures to high waves. To investigate potential damage to rubble mounds, both hydraulic model experiments and numerical analyses have been used. Numerical analyses typically employ methods such as the finite element method or particle-based approaches, which can involve high computational loads. In this study, the authors focused on the similarity between the damage process of rubble mounds and advection-diffusion phenomena, initiating repeatability calculations using analytical solutions of advection-diffusion equations. Results from hydraulic model experiments revealed clear relationships between diffusion coefficients and advection velocities, based on wave conditions and mound conditions. This insight enabled the determination of advection velocities and diffusion coefficients from the given wave and mound conditions. Therefore, an attempt was made to simulate the damage process of rubble mounds using advection-diffusion equations. The height reduction of the rubble mound's crest was effectively reproduced; however, challenges remained, as the calculated results tended to underestimate the slope profile on the offshore side.

Keywords: analytical solution; water flume experiment.

Introduction

Coastal structures that include rubble mound breakwater come in various types, such as rubble mounds alone, slope-protection breakwaters covered with armor blocks or concrete facing, and breakwaters covered with wave-dissipating blocks. During construction, these structures may temporarily exist only as rubble mound before reaching the final cross-sectional shape. Especially for offshore airports, it is common practice to first construct a rubble-mound perimeter, followed by subsequent landfilling.

The construction sequence for reclamation projects was shown in Figure 1: firstly, the groundwork is laid by building the sand bed (step 1) and rubble mound (step 2), and the perimeter of the reclamation site is established in advance, as shown in phase a. Once a considerable portion of the perimeter is built, phase b proceeds with construction caissons and superstructures (step 3), placing amor stones or amor blocks (step 4), and installing was wave-dissipating blocks (step 5). However, due to the need to complete phase a before moving on to phase b, the rubble mound remains exposed until the latter phase is finished. During this period, there is a risk that high waves caused by typhoons or other storms could damage the exposed rubble mound, a recurring issue on construction sites.

As a countermeasure, filter units are often used to cover the rubble mound, yet as shown in Photo 1, there have been instances of damage to both the rubble mound and filter units caused by high waves. Other countermeasures have been proposed by Fukumizu et al.(2017) and Sakai et al. (2020), who have developed unique damage-reduction measures through hydraulic model experiments. However, challenges remain with site applicability, and these proposals have yet to be implemented on-site.

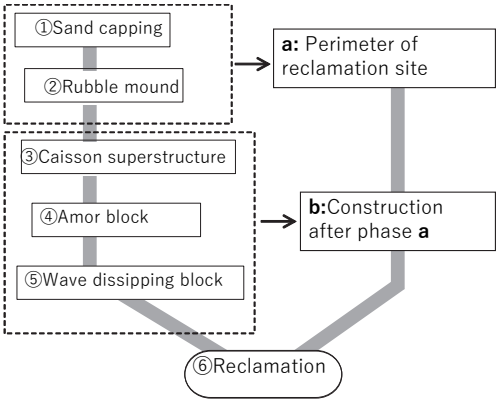

Figure 1. Construction sequence for reclamation project

[1] Toyo Construction Co. Ltd., Naruo Research Institute, 1-25-1, Naruohama, Nishinomiya, 663-8142, Japan, sakai-daiki@toyo-const.co.jp.

[2] Toyo Construction Co. Ltd., Naruo Research Institute, 1-25-1, Naruohama, Nishinomiya, 663-8142, Japan, tsujimoto-gozo@toyo-const.co.jp.

Photo 1 Damage of filter units due to high waves

Araki et al. (200) conducted numerical simulations to reproduce damages to rubble mounds using coupled calculations of wave transformation based on nonlinear dispersive wave equations the Discrete Element Method (DEM), while Fukumizu et al.(2018) attempted to perform similar coupled calculations using CADMAS-SURF with DEM. Although rubble mounds were not the target, Goto et al.(2013) used particle methods to simulate the destruction of the rubble mound on composite breakwaters caused by overtopping. However, these analytical approaches are expected to have high computational loads.

In response, Sakai et al.(2022) attempted to reproduce the damage process of rubble mounds by numerically solving advection-diffusion equations. However, they did not develop aa general method for setting advection velocities and diffusion coefficients. This study, therefore, aims to reproduce the damage processes of rubble mounds using the advection-diffusion equation's analytical solution, incorporation advection terms based on the results of hydraulic model experiments by Sakai et al.(2020a, 2020b) The goal is to evaluate advection velocities and diffusion coefficients from wave and mound conditions.

Experimental approach

The hydraulic model experiments were conducted using a two-dimensional wave flume owned by the Naruo Research Institute of Toyo Construction Co,Ltd. The flume measures 40 m in length, 2.0m in height, and 1.0m in width (Figure 2). A piston-type wave generator was used, with a model scale of 1/25, and the rubble mound model, as shown in Figure 3, was formed with crushed stones with a median diameter of 1.3 cm and an average mass of 3.4 g. The water depth was set at 28 cm above the temporary floor, matching the initial crest height d_o.

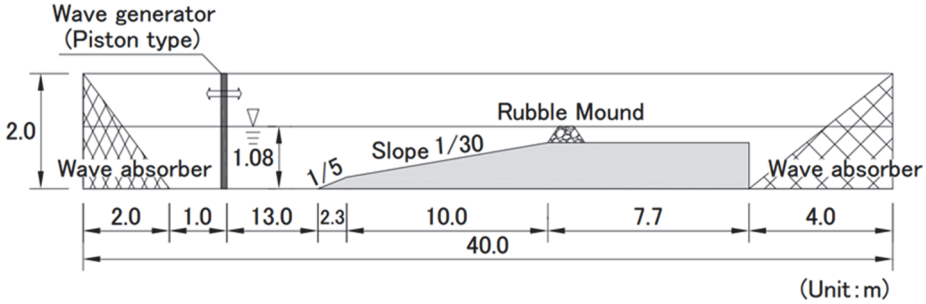

Figure 2 Two-dimensional wave flume

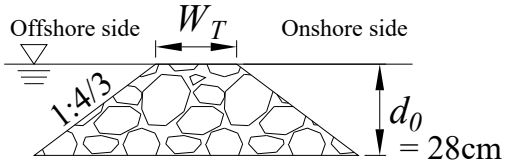

Figure 3 Rubble mound model

Irregular waves, generated according to a modified Bretschneider-Mitsuyasu spectrum, were applied. The experiment consisted of 36 cases, covering significant wave height $H_{1/3}$=10,12,14, cm (field-scale equivalents: 2.5, 3.0, 3.5 m), the significant wave periods $T_{1/3}$ =2.0, 2.5, 3.0 second (field-scale equivalents: 10.0, 12.5, 15.0 second), and crest widths W_T =12, 24, 36, 48 cm (field-scale equivalents: 3, 6, 9, 12 m). Each case had a wave action duration of 4.8 hours, corresponding to 24 hours at field scale.

An example of the damage process observed in the hydraulic model experiments is shown in Figure 4. Over time, the crest height is decreasing, with many stones on the crest shifting toward the onshore side. Van der Meer et al.(1994) conducted similar hydraulic model experiments with submerged crest conditions and reported similar damage processes.

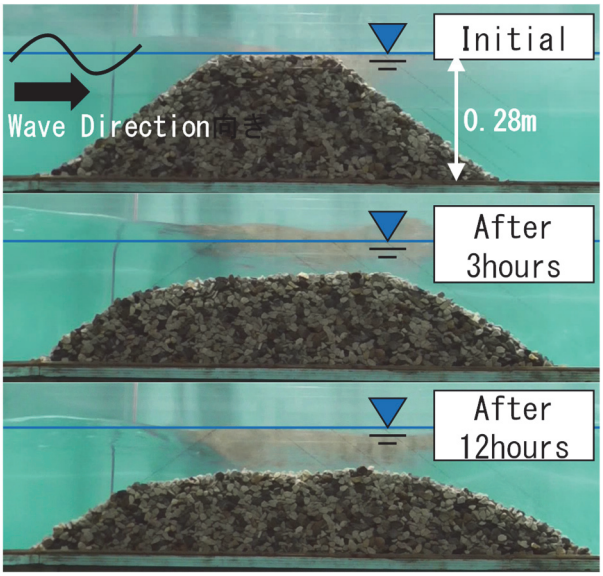

Figure 4 Damage processes of rubble mound model

Figure 5 shows a sample of the experimental results under conditions $H_{1/3}$=14 cm, $T_{1/3}$=2.0 s, W_T=12 cm. In the experiment, the profile was measured at hourly intervals (field-scale equivalents). A significant crest lowering was observed during the first hour, with stones being transported to the lower part of the onshore slope. Subsequently, stones on the crest were gradually transported toward the onshore side. On the offshore side, only slight movement of stones toward the offshore slope was observed, with minimal loss of stone offshore. These trends were consistent across other experimental cases.

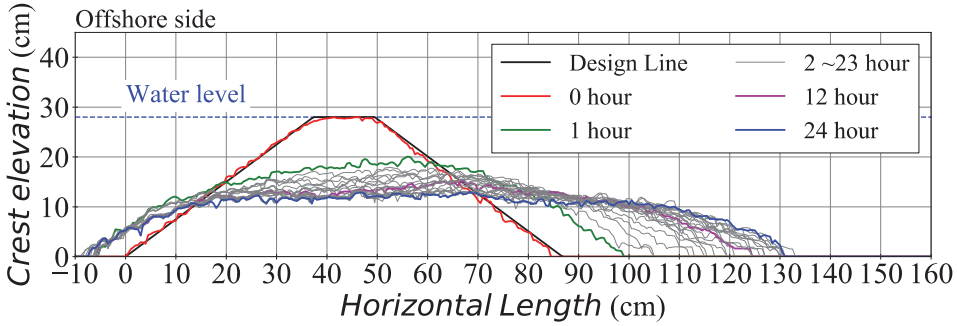

Figure 5 Shape changes of rubble mound model

Optimum values of advective velocity and diffusion coefficient

We focused on the similarity between the shape changes of rubble mounds and the shoreline changes of nourished beaches. Todd L Walton Jr. (1994) clarified the changes in beach nourishment shapes, as shown in Figure 6, using the analytical solution of the diffusion equation. Here, we conducted an analysis (Eq. (1)) using a newly derived analytical solution that includes an advection term. The variables of eq. (1) are shown in Figure 6.

$$\frac{y(x,t)}{d} = \frac{1}{2}[\mathrm{erf}(AX+A) - \mathrm{erf}(AX-A)] + \frac{1}{2}\left(\frac{B-AX}{B-A}\right)[\mathrm{erf}(AX-A) - \mathrm{erf}(AX-B)] + \frac{1}{2}\left(\frac{B+AX}{B-A}\right)[\mathrm{erf}(AX+A) - \mathrm{erf}(AX+B)] + \frac{1}{2\sqrt{\pi}(B-A)}\{\exp[-(AX-B)^2] - \exp[-(AX-A)^2]\} + \frac{1}{2\sqrt{\pi}(B-A)}\{\exp[-(AX+B)^2] - \exp[-(AX+A)^2]\} \quad (1)$$

Where $A = \alpha/\sqrt{4\nu t}$, $B = \beta/\sqrt{4\nu t}$, $A = (x - Ct)/\alpha$, erf is error function, C is advection velocity and ν is diffusion coefficient. Both of C and ν are unknown value. By substituting the shape results of the rubble mound from the hydraulic model experiments into Equation (1). The values of C and ν were calculated by the nonlinear least squares' method.

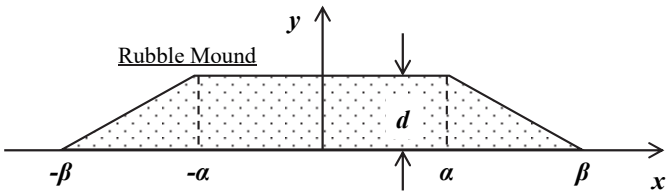

Figure 6 Variables of rubble mound model

Figure 7 shows a sample time series of the dimensionless diffusion coefficient. The vertical axis is the dimensionless diffusion coefficient, which is normalized using the crest width W_T of the rubble mound and significant wave period $T_{1/3}$. The horizontal axis shows the wave action time, normalized by $T_{1/3}$. The dimensionless diffusion coefficients fit well with the power approximation $y = 0.679x^{-0.492}$, with a determination coefficient of R=0.976, indicating a good correlation with wave characteristics.

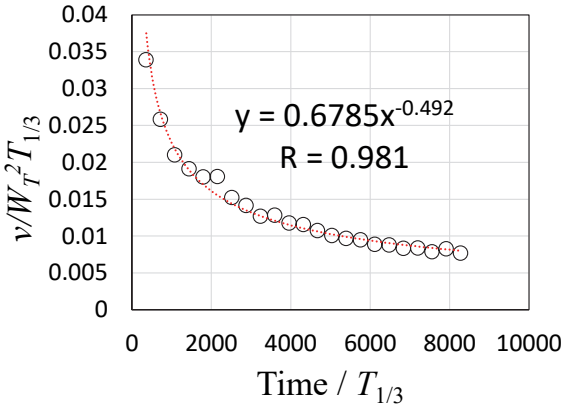

Figure 7 Time series of dimensionless diffusion coefficient

Figure 8 presents an example of time series of the dimensionless advection velocity, which is normalized using W_T and. significant wave height $H_{1/3}$. Like the dimensionless diffusion coefficient, the dimensionless advection velocities fit well with a power approximation $y = 0.284x^{-0.609}$,yielding a high correlation R=0.976.

The calculated values of the diffusion coefficient ν and advection velocity C show a strong correlation with wave characteristics. To further clarify this relationship, coefficient a and b for the power approximation $y = ax^b$ were calculated for all 36 cases under the hydraulic model experiment

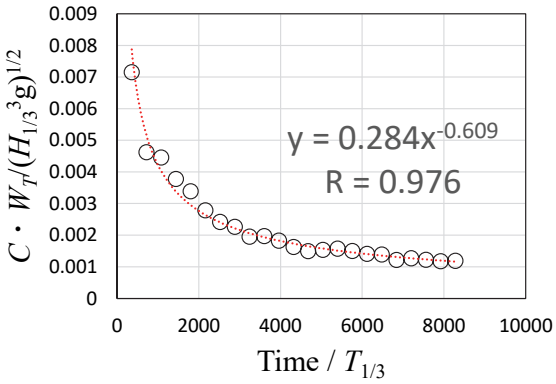

Figure 8 Time series of dimensionless advection velocity

conditions. Figure 9 and 10 illustrate the relationship between coefficient a and b for the dimensionless diffusion coefficient and a modified Ursell number (hereafter, U_r), defined using crest width W_T and wavelength L, according to Eq. (2). For coefficient a, the relationship $a = 0.559U_r^{1.958}$ was obtained, while for coefficient b, $b = -0.122\ln(U_r) - 0.509$ provided a relatively high correlation.

$$Ur = \sqrt{\left(\frac{H_{\frac{1}{3}}}{L}\right)^2 \left(\frac{W_T}{L}\right)^3} \tag{2}$$

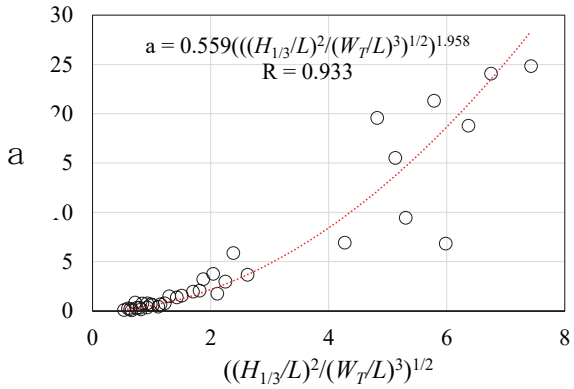

Figure 9 Relationship between a and Ur for dimensionless diffusion coefficient

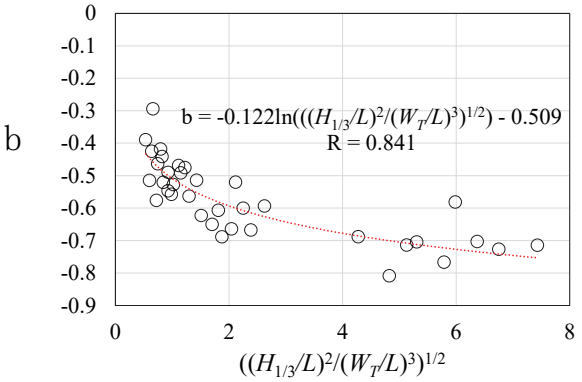

Figure 10 Relationship between a and Ur for dimensionless diffusion coefficient

Similarly, Figure 11 and 12 display the relationship between coefficient a and b for the dimensionless advection velocity and U_r. While coefficient a follows the relationship $a = 0.536U_r^{-1.349}$, coefficient b did not show a high correlation. Due to the relatively small variation in coefficient b across experimental case, it was assigned a constant value (-0.6) in this study.

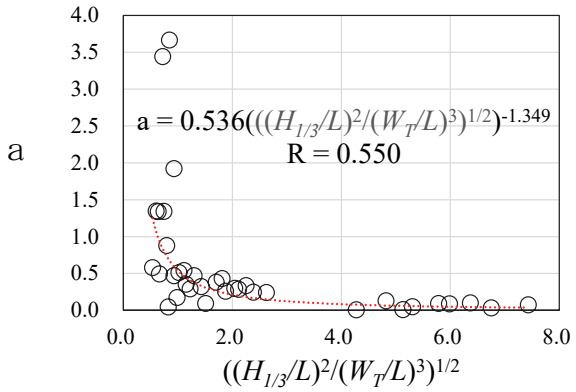

Figure 11 Relationship between a and Ur for dimensionless advection velocity

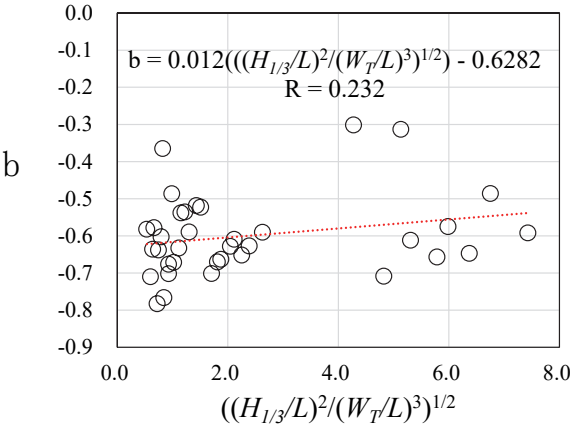

Figure 12 Relationship between b and Ur for dimensionless advection velocity

Therefore, the dimensionless diffusion coefficient is given as Eq.(3) and the dimensionless advection velocity Eq.(4).

$$\frac{\nu \cdot T_{\frac{1}{3}}}{W_{T^2}} = 0.559U_r^{1.955}\left(\frac{t}{T_{\frac{1}{3}}}\right)^{-(0.122U_r+0.509)} \tag{3}$$

$$\frac{C \cdot W_T}{\sqrt{H_{\frac{1}{3}}^3 g}} = 0.536U_r^{-1.349}\left(\frac{t}{T_{\frac{1}{3}}}\right)^{-0.6} \tag{4}$$

where g is gravitational acceleration and t is a wave action duration.

Example of rubble mound damage simulation

Based on the above findings, dimensionless advection velocity and diffusion coefficient can now be calculated from wave and mound conditions. Figure 13 compares the analytical and experimental results of the rubble mound's damage shape after 24 and 48minutes under wave height of 10 cm, wave period of 2.5 s, and crest width of 10 cm. The height of the crest was reproduced with high accuracy. However, differences were observed in the offshore slope shape; according to experimental observations, individual

stones on the offshore slope tended to slide or roll, moving not as a collective mass but as individual units, which likely contributed to the discrepancy between the analytical and experimental results.

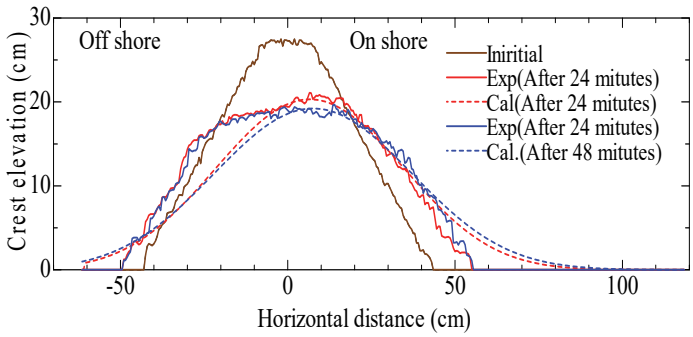

Figure 13 Comparison between analytical and experimental results

Conclusions

The primary findings from this study are as follows:

1. Dimensionless diffusion coefficient and advection velocity were calculable based on a modified Ursell number, defined using crest width and wavelength.

2. The damage process of the rubble mound was well reproduced with respect to the decrease in crest height.

3. The calculated offshore slope shape was underestimated, likely due to the distinct behavior of individual stones observed in experiments, which suggests movement behavior different from typical advection-diffusion phenomena. This discrepancy remains a topic for further study.

REFERENCES

Araki, S., Fujiwara, Y., Miyazaki, T. and Deguchi, I., 2000. Calculation of cross-sectional deformation of rubble mound breakwater using the discrete element method, *Coastal Engineering.*, *JSCE*, Vol. 47, pp. 761-765, (in Japanese).

Fukumizu, K., Sakai, D., Kanazawa, T. and Araki, S., 2017. Fundamental study on countermeasure against deformation of rubble mound seawall under construction, *Ser. B2* (*Coastal Engineering.*), *JSCE*, Vol. 73, No. 2, pp. I_1105-1110, (in Japanese).

Fukumizu, K., Sakai, D., Kanazawa, T. and Araki, S., 2018. Development of Effective Technique on Rubble Mound Seawall in Artificial Island Under Construction, *Proceedings of the 28th International Offshore and Polar Engineering Conference, ISOPE*, Vol. III, PP.1197-1202, 2018

Goto, H., Ikari, H., Haraguchi, K., Nakajima, H. and Tonomo, K., 2013: Development of Numerical Wave Flume by Particle Method for Simulating Tsunami-Overtopping induced Failure of Composite Breakwater and its Prevention Work, *Ser. B2* (*Coastal Engineering.*), *JSCE*, Vol. 69, No. 2, pp. I_881-885, (in Japanese).

Sakai, D., Kanazawa, T. and Tsujimoto, G., 2019. Basic study on the damage process in the middle of the construction of rubble mound by waves, *Ser. B2* (*Coastal Engineering.*), *JSCE*, Vol. 75, No. 2, pp. I_925-930, (in Japanese).

Sakai, D., Kanazawa, T. , Kanda, T. and Tsujimoto, G., 2020a. A study on damage reduction measures focusing on rubble mound during construction, *J. JSCE*, *Ser. B3* (*Ocean Eng.*), Vol. 76, No. 2, pp. I_522-I_527, (in Japanese)

Sakai, D., Tsujimoto, G., Kanazawa, T. and Kanda, T., 2020b. A Study on the Damage Characteristics of Rubble Mound During Construction by Waves, *Ser. B2* (*Coastal Engineering.*), *JSCE*, Vol. 76, No. 2, pp. I_925-930, (in Japanese).

Sakai, D. and Tsujimoto, G., 2022. Proposal on a new simple method for reproducing deformation processes of rubble mound profiles, *Proceedings of the 32th International Offshore and Polar Engineering Conference, ISOPE*, PP.2769-2774.

Todd L. Walton Jr., 1994. Shoreline Solution for Tapered Beach Fill, *Journal of Waterway, Port*, *Coastal*, *and Ocean Engineering*, Vol. 120, Issue 6, pp.651-655.

Van der Meer, J.W. and Daemen, I. F. R., 1994. Stability and wave transmission at low-crested rubble-mound structures, *Journal of Waterway, Port, Coastal, and Ocean Engineering*, Vol. 120, No.1, PP.1-19.